

LOW-ENERGY ION OUTFLOWS FROM THE IONOSPHERE DURING A MAJOR POLAR CAP EXPANSION — EVIDENCE FOR EQUATORWARD MOTION OF INVERTED-V STRUCTURES

M. Lockwood,* A. P. van Eyken,** B. J. I. Bromage,* J. H. Waite, Jr,***
T. E. Moore*** and J. R. Doupnik†

*Rutherford Appleton Laboratory, Chilton, Didcot, OX11 0QX, U.K.

**Millstone Hill Radar, MIT Haystack Observatory, Westford, MA 01886, U.S.A.

***NASA/Marshall Space Flight Center, Huntsville, AL 35812, U.S.A.

†Center for Atmospheric and Space Sciences, Utah State University, Logan,
UT 84322-3400, U.S.A.

ABSTRACT

Data from the Dynamics Explorer 1 satellite and the EISCAT and Sondrestrom incoherent scatter radars, have allowed a study of low-energy ion outflows from the ionosphere into the magnetosphere during a rapid expansion of the polar cap. From the combined radar data, a 200kV increase in cross-cap potential is estimated. The upflowing ions show "X" signatures in the pitch angle-time spectrograms in the expanding midnight sector of the auroral oval. These signatures reveal low-energy (below about 60eV), light-ion beams sandwiched between two regions of ion conics and are associated with inverted-V electron precipitation. The lack of mass dispersion of the poleward edge of the event, despite great differences in the times of flight, reflects the equatorward expansion of the acceleration regions at velocities similar to those of the antisunward convection. In addition, a transient burst of upflow of O^+ is observed within the cap, possibly due to enhanced Joule heating during the event.

INTRODUCTION

The study of low-energy ion flows from the ionosphere into the magnetosphere under time-varying conditions is made very difficult by the spatial/temporal ambiguity of satellite data, the main source of information on such outflows (see /1/ for review). Various mechanisms for transient O^+ ion outflows have been proposed /2, 3/ but observations of such effects are rare. Farmer et al /4/ have found that the topside ionosphere contains enhanced upward flows in response to substorms by using incoherent scatter data, which do not suffer from the spatial/temporal ambiguity problem.

In this paper, ion outflows are studied using the RIMS experiment on DE1 (see /1/) during a major expansion of the polar cap. The cap behaviour is monitored by simultaneous observations by the EISCAT and Sondrestrom incoherent scatter radars. The main outflow feature discussed is an "X-event", first reported by Moore et al /5/. In these events an upgoing ion beam is sandwiched between two conics, giving an X-shaped form to the RIMS spin angle-time spectrograms. Data from earlier in the DE mission allow comparison of RIMS and HAPI data (see /1/) and show that upgoing, X-event ions are co-located with inverted-V electron precipitation signatures /6, 7/ and with shear-like polar cap boundary convection reversals /8/. The co-location of X-events, inverted-V events and the convection reversals strongly suggests that they are the result of a field-aligned electric field structure : in addition to giving the upgoing ion beam at the centre of the event, such a structure can give transverse acceleration, and hence conics, at its edges /7, 9, 10/. Note that such an explanation requires that the field-aligned electric field extended to below the satellite.

Unfortunately, no simultaneous observations of precipitating electrons are available during the polar cap expansion studied in this paper. By the date of these observations (February 3rd, 1984), the HAPI instrument was no longer operational. However, DC electric fields were measured by the Plasma Wave Instrument (PWI) on DE1. In this paper, therefore, inverted-V events are not observed directly from precipitating electrons, rather they are inferred from the upgoing ion X-event signature.

RADAR OBSERVATIONS OF THE POLAR CAP EXPANSION

The co-ordinated 24-hour run of the EISCAT and Sondrestrom incoherent radars on February 3rd, 1984 will be discussed in detail by van Eyken et al /11/. Both radars employed beam-swinging techniques to determine plasma drift velocities at points well removed from the radar locations /12, 13/.

The Polar Cap Expansion Between 12:20 and 20:16 UT

The EISCAT observations, using UK Special Programme POLAR /12, 13/, are summarised in Figure 1. The outer band shows 10-minute averages of the 2.5-minute resolution convection vectors. A full description of the data presentation format is given in /13/. An interesting change in the convective flows is observed throughout the field of view ($\Lambda=70-75^\circ$) near 22:00 MLT, shortly after EISCAT has rotated under the Harang discontinuity: the newly-established eastward flows swing abruptly south westward. This change is shown in greater detail by the 2.5-minute resolution vectors in figure 2b.

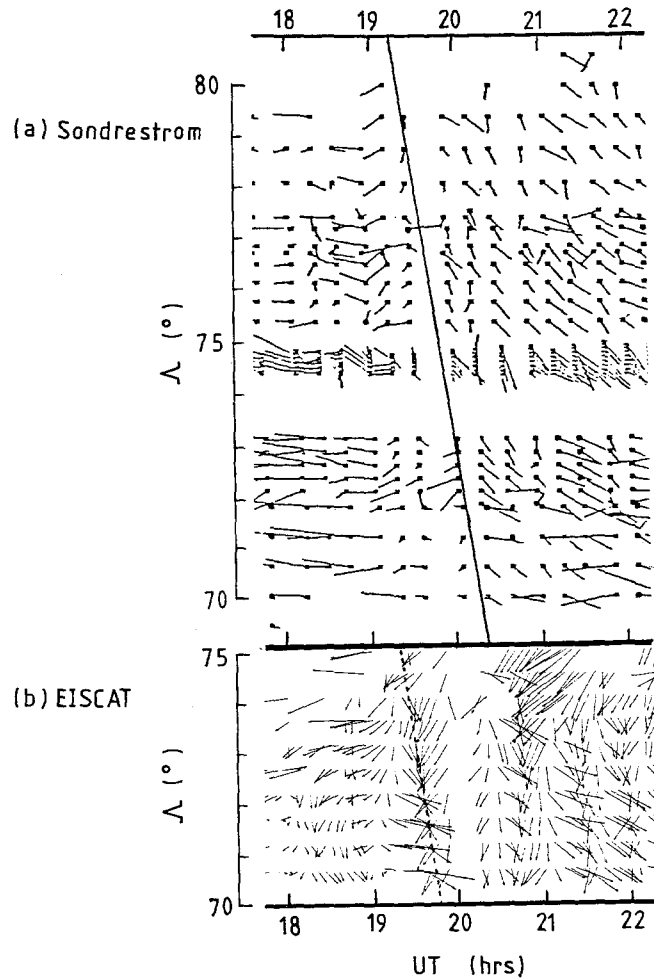


Fig. 2. Field-perpendicular convection vectors observed by the (a) Sondrestrom and (b) EISCAT radars as a function of invariant latitude, Λ for the period around the convection enhancement. The boundaries denoted by the solid and dashed lines are interpreted as the polar cap boundary at Sondrestrom and EISCAT respectively.

At the time of this change (near 19:30 UT), Sondrestrom is near 16:00 MLT. A major convection change is also observed in the Sondrestrom data, with a swing from the usual westward sub-auroral afternoon flows through southward to eastward. The eastward flows then persisted for 4 hours /11/. Figure 2a shows that the reversal occurs throughout the field of view ($\Lambda=70-80^\circ$) within two latitude scan periods of the Sondrestrom radar, i.e. within 50 minutes.

The only explanation for these data from both radars is that the polar cap has expanded and placed both fields of view in the polar cap /11/. It is interesting and important to note that the data from either radar without the other would have been open to serious misinterpretation. Figure 2 shows that the polar cap boundary moves to lower Λ at both locations at an approximately constant rate.

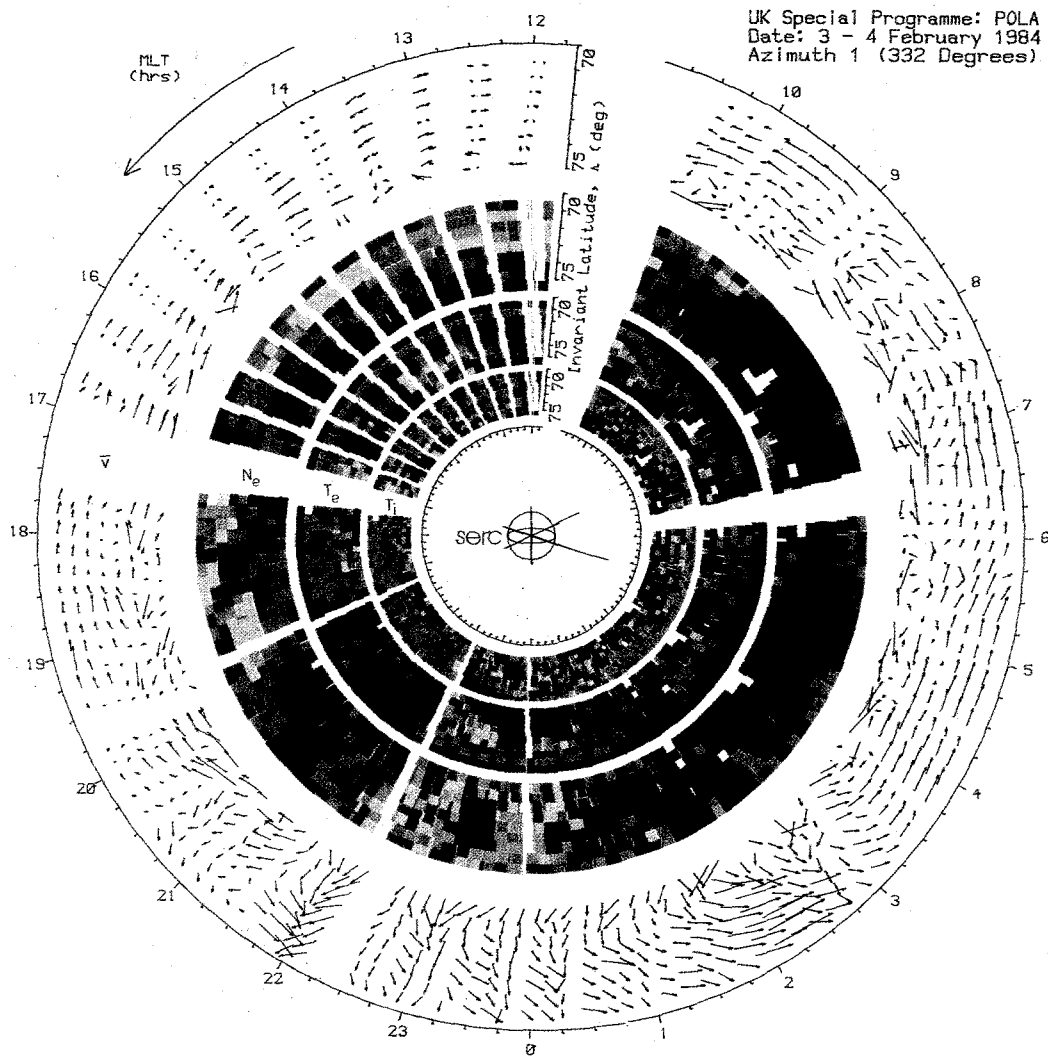


Fig. 1. Concentric MLT-invariant latitude polar dial plots of EISCAT observations on 3-4 February, 1984. From the outer band inwards: (a) the field perpendicular velocity vectors, \vec{V} ; (b) the plasma density, N_e ; (c) the electron temperature T_e ; and (d) the ion temperature, T_i . The invariant pole is at the centre for each plot. A major convection enhancement is observed near 22:00 MLT, corresponding to 19:30 UT.

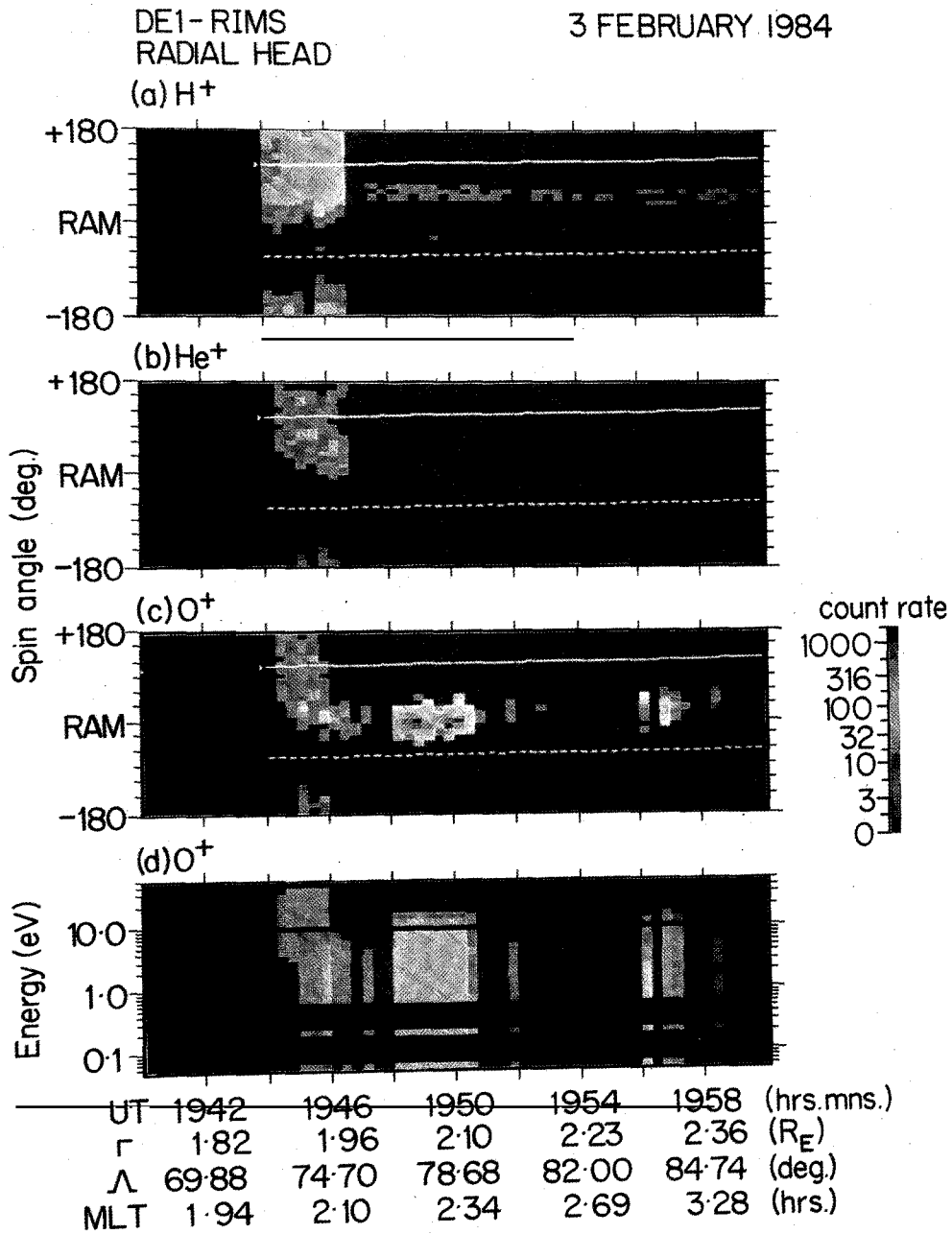


Fig. 4. Spectrograms from DE1-RIMS radial head during the cap expansion (a), (b) and (c) are spin angle-time spectrograms for H⁺, He⁺ and O⁺ respectively. (d) shows the energy-time spectrogram for O⁺.

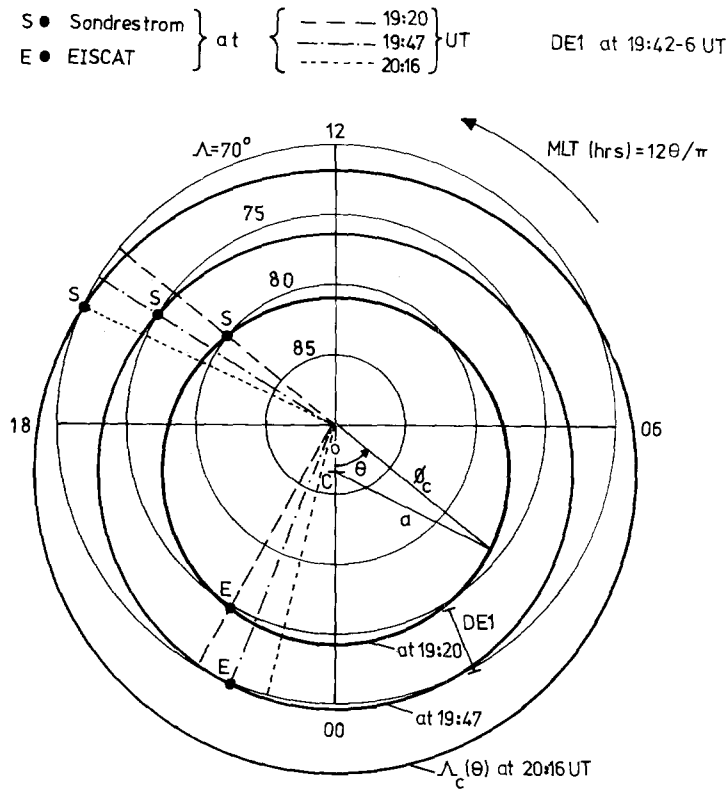


Fig. 3. Polar cap boundary locations at Sondrestrom (S) and EISCAT (E) for three Universal Times (UT = 19:20; 19:47 and 20:16) and as seen by Dynamic Explorer 1 (DE1) between 19:42 and 19:46 UT. The circles are fits to the radar data, centred on the point C.

The locations of the polar cap boundary seen by the two radars are shown in Figure 3 for various UT. It can be seen that these can be fitted by an expanding circular polar cap, centred at the point C (offset from the invariant pole towards midnight by 3°). The use of a circular form is obviously a gross extrapolation as no data are available for the entire dawn sector. However, DE1 was moving into the cap at this UT, along a meridian near 02:00 MLT. When it encountered the cap boundary the convection signature was highly complex with several reversals from eastward to westward. However, before 19:42 UT the convection observed by DE1-PWI was strongly eastward, after 19:46 UT it was westward. Hence the error bar shown in Figure 3 denotes the possible spread in the location of the cap boundary, i.e. DE1 places the cap boundary slightly to the north than is predicted by the circular extrapolation.

The Cross Cap Potential Increase

The rate of expansion of the cap is directly related to the cross-cap potential increase required to cause the expansion if no tail reconnection is occurring /14, 15/. The circular cap expansion shown in Figure 3 calls for a 200 kV increase in cross cap potential. The DE1-PWI evidence suggests that the cap may have been slightly deformed from circular and not expanding as rapidly in the dawn sector as it is in the dusk; consequently this cap potential may be an over-estimate. On the other hand, the cap boundary at EISCAT has an expansion speed of 0.4 kms⁻¹, whereas Figure 2 shows the southward velocities to be near 0.7 kms⁻¹. The flow of 0.3 kms⁻¹ across the boundary indicates reconnection in the tail, i.e. magnetic flux being taken out of the polar cap at the MLT of EISCAT. DE1 sees only the high-altitude equivalent of the 0.4 kms⁻¹ cap expansion flow. If reconnection of the rate observed at EISCAT extended over 4 hours of MLT, this would add another 30kV to the cross cap potential required.

A cross cap potential of 200kV is large, Reiff et al /16/, for example, observed a range of values up to 170kV and Lockwood et al /15/ have observed the early expansion of a new

convection pattern and polar cap following a southward turning of the IMF which caused an increase in cross potential of 140kV. There is, however, some evidence that the value of 200kV is roughly correct. For this value and the circular cap expansion shown in Figure 3, the cross-cap transit time from the original cleft location to the EISCAT field of view is computed to be 47 minutes. Figure 1 shows that 47 minutes after the estimated start of the cap expansion, very high density plasma is seen by EISCAT, in fact higher densities than those observed on the dayside. Cross-correlation analysis of data from the two azimuths shows that these high densities are arriving at the nightside, and are not a static feature in an MLT- Λ frame under which the radar is rotating (see /15/). The transit times for the high density plasma to convect over the polar cap is consistent with the estimated 200 kV increase in cap potential.

ION FLOWS OBSERVED BY DE1-RIMS

Within the structured electric field region around the cap boundary, shown in Figure 3, RIMS observes the upgoing X-event shown in Figure 4. The instrument was only turned on at 19:44 UT, just in time to observe the rapid cap expansion. The H^+ and He^+ spin angle-time spectrograms show clear X signatures, with the upgoing beam at the centre pulled towards the RAM direction, a sign of a strong headwind, as observed by PWI. For this reason, the X-signature is not clear in the O^+ data, as in the case discussed by Moore *et al* /5/. The RIMS Z heads show strong fluxes near the edges of the event, with an abrupt cutoff at 19:47 UT for all 3 ion species. The temperature of these ions, obtained by fitting Maxwellian distributions to Z head energy spectrograms, falls continuously as DE1 moves poleward through the event and the ion density rises (see Figure 5). The fall in O^+ energy is also seen in the energy spectrogram for O^+ from the radial head (Figure 4d). Particular attention is drawn here to the lack of any spatial dispersion of the event boundaries and centre between ion flows of different mass.

Note that once within the cap proper RIMS observes a short burst of low energy (<10eV) O^+ ions which are rammed by the combined action of the spacecraft motion and the convection headwind.

Time of Flight Considerations

No time-of-flight dispersion is expected for static X-events as they are located on largely east-west convection reversals and DE1 flies through them in a north-south direction. Hence the convection component along the spacecraft orbit is small and no dispersion effects are to be expected. However, in this case there is a component of convection along the orbit of 1.1 kms^{-1} (equivalent to 0.4 kms^{-1} at ionospheric altitudes), due to the rapid expansion of the polar cap, yet still no dispersion is observed. The source of the ions is fairly narrow (roughly 5° of invariant latitude) and hence, if it were stationary, energy dispersion would be expected by the geomagnetic mass spectrometer effect /17/, as observed in the cleft ion fountain on the dayside (see /1/). However, this would give increasing energy as DE1 moved poleward, as the convection component along the orbit plane is equatorward. Figures 4 and 5 show the opposite to be the case, which must therefore reflect a spatial or temporal change in the strength of ion heating.

The poleward edge of the X-event was observed within 8 seconds of 19:46:36 UT by all mass channels of the Z heads. The radial head also observed the poleward edge for H^+ and He^+ at this time, although cold rammed O^+ is seen for another 32 seconds. This defines the poleward edge of the event to be at the same invariant latitude for all 3 ion species to within $\Delta\Lambda=0.18^\circ$. If the times of flight for 2 species (from source to satellite) differ by Δt seconds, this limits the difference between the convection velocity and the source velocity (V_C and V_S respectively) according to the inequality

$$\Delta V = (V_S - V_C) < \frac{\Delta\Lambda}{\Delta t} d \quad (1)$$

where V_S and V_C are measured at ionospheric altitudes where the distance d along the orbit plane is equivalent to 1 degree of Λ .

In order to compute the times of flight for each ion species, it is necessary to know the pitch angle, the energy and hence the spacecraft potential. Due to the effect of the spacecraft motion, the O^+ pitch angle cannot be resolved by the radial head, however comparison of the T_{\parallel} of 3eV observed by the radial head with the T_{\perp} of 1.9eV observed by the Z heads, gives an estimate of the O^+ pitch angle peak of 140° at the poleward edge of the event. This compares with values of 130° and 110° observed by the radial head for H^+ and He^+ respectively. The spacecraft potential is not accurately known, however at altitudes near $2R_E$ the value is typically +1eV (sufficient to exclude the classical polar wind). Using this value, the conic energies at DE1 for the poleward edge of the event are

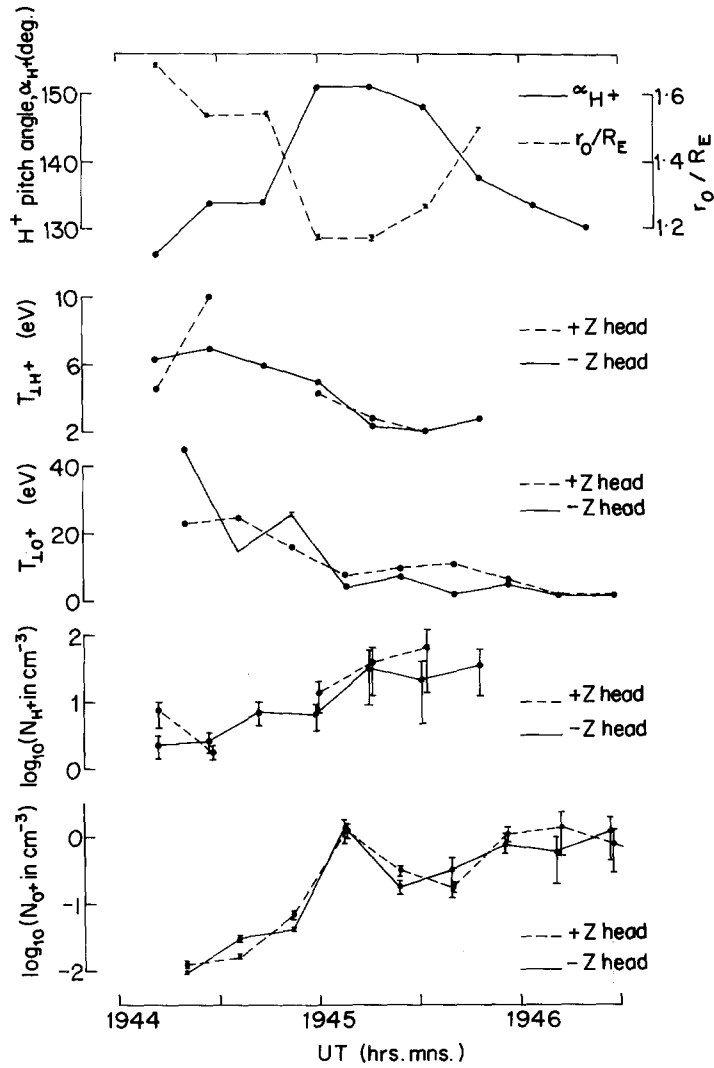


Fig. 5. The X-event, as seen by the radial head of RIMS in the H⁺ pitch angle peak, α_{H^+} and geocentric distance of the source, r_0 , computed assuming adiabatic motion. Also shown are the H⁺ and O⁺ transverse temperatures $T_{\perp H^+}$ and $T_{\perp O^+}$ and ion densities N_{H^+} and N_{O^+} deduced from Maxwellian fits to the -Z (solid lines) and +Z (dashed lines) heads of RIMS.

6eV, 5eV and 4.5eV for H⁺, He⁺ and O⁺ respectively. The times of flight for such low energy ions are large; if adiabatic motion is assumed following initial transverse acceleration (using the equation given in /19/), the difference between the value for O⁺ and H⁺ is at least 660 seconds. Hence from equation (1), the source and convection velocities must differ by less than $\Delta V = 0.03 \text{ kms}^{-1}$. Any larger value of ΔV would cause mass dispersion of the poleward edge of the event.

This maximum value for ΔV must be compared with an ionospheric convection velocity of 0.4 kms^{-1} , the value being even higher at the source altitude. Hence the lack of mass dispersion of the edge of the upgoing ion signatures indicates that the source is moving with the convection velocity: the convection velocity component along the orbit is 0.4 kms^{-1} and the same component of the source velocity is $0.4 \pm 0.03 \text{ kms}^{-1}$. The radar and DE1 data convection data have shown that the cap boundary is moving at the convection speed at the location of DE1, i.e. no reconnection is occurring at that MLT and DE1 encounters

an "adairoic" cap boundary /15/. Hence these data identify the X-event ion source and the cap boundary to be moving together during this polar cap expansion.

O⁺ Flows Within the Cap

The O⁺ flows seen after 19:48 UT, within the polar cap, could have originated from the cleft ion fountain /1/ and been convected by the increased convection field. The enhancements of thermal plasma seen in the nightside auroral oval by EISCAT are consistent with this idea. The suprathermal O⁺ seen by RIMS, however, is observed too soon (by several tens of minutes) for this to be the case. In addition the cleft ion fountain flows would have been observed throughout the cap (instead of ceasing at 19:51 UT) and would have displayed energy dispersion effects. This points to an ionosphere source for this transient burst of O⁺ flow which lies within the polar cap. One possible explanation of this is an upflow induced by increased Joule heating due to the enhanced convection speeds accompanying the polar cap expansion, as recently modelled by Gombosi *et al* /3/ and detected in the ionospheric F-region by Winsor *et al* /18/. Similarly Farmer *et al* /4/ have observed topside ion outflows following substorms, which could also be attributed to the associated joule heating increase.

CONCLUSIONS

The lack of mass dispersion of upgoing ion X-events, even during a major polar cap expansion (equivalent to a cross-cap potential increase of order 200kV), indicates that X-event sources move with the cap boundary. The association of X-events with inverted-V electron precipitation features suggests that inverted-V structures may move with the cap boundary also, although it must be stressed that it is only the upgoing ion source which has been observed to move in these data. The major increase in the convection strength also appears to cause a burst of suprathermal (up to 10eV) O⁺ outflow from the polar cap ionosphere.

REFERENCES

1. M. Lockwood, Low-energy ion flows into the magnetosphere, this issue.
2. N. Singh and R.W. Schunk, Temporal behavior of density perturbations in the polar wind, J. Geophys. Res., 90, 6487 (1985).
3. T.I. Gombosi, T.E. Cravens and A.F. Nagy, A time-dependent theoretical model of the polar wind: preliminary results, Geophys. Res. Lett., 12, 167 (1985).
4. A.D. Farmer, M. Lockwood, R.B. Horne, B.J.I. Bromage and K.S.C. Freeman, Field-perpendicular and field-aligned plasma flows observed by EISCAT during a period of prolonged northward IMF, J. atmos. terr. Phys., 46, 473 (1984).
5. T.E. Moore, C.R. Chappell, M. Lockwood and J.H. Waite, Jr., Superthermal ion signatures of auroral acceleration processes, J. Geophys. Res., 90, 1611 (1985).
6. D.W. Swift, Mechanisms for Auroral precipitation: A review, Rev. Geophys. and Space Phys., 19, 185 (1981).
7. F.S. Mozer, C.A. Cattell, M.K. Hudson, R.L. Lysak, M. Temerin and R.B. Torbert, Satellite measurements and theories of low altitude auroral particle acceleration, Space Sci. Rev., 27, 155 (1980).
8. R.A. Heelis and W.B. Hanson, High latitude convection reversals in the Nighttime F Region, J. geophys. Res., 85, 1995 (1980).
9. M.E. Greenspan, Effects of oblique double layers on upgoing ion pitch angle and gyrophase, J. geophys. Res., 89, 2842 (1984).
10. J.E. Borovsky and G. Joyce, Numerically simulated two-dimensional auroral double layers, J. geophys. Res., 88, 3116 (1983).
11. A.P. van Eyken, private communication (1986).
12. A.P. van Eyken, H. Rishbeth, D.M. Willis and S.W.H. Cowley, Initial EISCAT observations of plasma convection at invariant latitudes 70-77°, J. atmos. terr. Phys., 46, 635 (1984).
13. D.M. Willis, M. Lockwood, S.W.H. Cowley, A.P. van Eyken, B.J.I. Bromage, H. Rishbeth, P.R. Smith and S.R. Crothers, A survey of simultaneous observations of the high-latitude Ionosphere and Interplanetary Magnetic Field with EISCAT and AMPTE-UKS, J. atmos. Terr. Phys., in press (1986).

14. M. Lockwood, A.P. van Eyken, B.J.I. Bromage, D.M. Willis and S.W.H. Cowley, Eastward propagation of a plasma convection enhancement following a southward turning of the Interplanetary Magnetic Field, Geophys. Res. Lett., 13, 72 (1986).
15. G.L. Siscoe and T.S. Huang, Polar cap inflation and deflation, J. Geophys. Res., 90, 543 (1983).
16. P.H. Reiff, R.W. Spiro, and T.W. Hill, Dependence of polar cap potential drop on interplanetary parameters, J. Geophys. Res., 86, 7639 (1981).
17. M. Lockwood, T.E. Moore, J.H. Waite, Jr., C.R. Chappell, J.L. Horwitz and R.A. Heelis, The geomagnetic mass spectrometer-Mass and energy dispersions of ionospheric ion flows into the magnetosphere, Nature, 316, 612 (1985).
18. K. Winsor, G.O.L. Jones and P.J.S. Williams, Variations in field-aligned plasma velocity with altitude and latitude in the auroral zone: EISCAT observations and the physical interpretation, Physica Scripta, in press (1986).